International Journal of Recent Technology and Engineering (IJRTE)
ISSN: 2277-3878 (Online), Volume-11 Issue-4, November 2022

RF and Shunt Active Power Filters at Multiple Points of Common Couplings of Radial Electrical Systems

Nor Farahaida Abdul Rahman

Abstract*: This work investigates the effects of RL filters and single-phase Shunt Active Power Filters (SAPFs) on the supply and load current waveforms and their properties. The parameters involved are rms, input Power Factor (PF) and Total Harmonic Distortion (THD). These parameters can describe the quality of any electrical power system, especially PF and THD. This work focuses on implementing both filters in an electrical radial system due to the limited research work. Hence, the effects of utilising both filters in the radial system are studied. In this work, both filters connect at different Points of Common Couplings (PCCs) of a single-phase radial electrical system. The PCCs are located before composite loads (Case 1), before all nonlinear loads (Case 1) and before individual nonlinear loads (Case 3). Both Cases 1 and 2 apply a centralised SAPF, and Case 3 employs individual SAPFs. Matlab/ Simulink simulates all case studies under four operating conditions: (1) without any filters, (2) with SAPFs only, (3) with RL filters only, and (4) with the RL filters and SAPFs. According to the simulation results, the SAPFs require the RF filters to compensate harmonic components effectively. Otherwise, the SAPF's injection current consists of high current spikes. However, the RF filters may slightly alter the load current waveforms, rms and THD values; the changes are insignificant. Moreover, based on the THD values of the compensated supply current waveform, the centralised SAPFs seem more suitable to be employed in the radial system. By utilising the centralised SAPFs, the THD values of the supply current are lower than using the individual SAPFs. Thus, it can be stated that the centralised SAPFs exhibit better performance. Nevertheless, connecting both filters on the PCCs of all nonlinear loads (Case 2) is suitable to avoid any linear load current waveform deterioration.

***Keywords*: Composite Loads, Linear Load, Nonlinear Load, Shunt Active Power Filters (SAPFs), Power Factor (PF), Total Harmonic Distortion (THD).**

I. INTRODUCTION

Electrical loads can be either linear or nonlinear loads. The elements of linear loads are resistors, inductors and capacitors only. Examples of linear loads are incandescent light bulbs and electric motors. Instead, nonlinear loads consist of a combination of semiconductor power converters and passive elements. Examples of nonlinear loads are computers, Adjustable Speed Drives (ASD) and LED lamps. The linear loads require a sinusoidal supply current waveform for their operation. However, inductive and capacitive linear loads can cause the phase angle of the supply current to lag or lead to the phase angle of the supply voltage waveform. Hence, it reduces the input Power Factor (PF). The low PF increases the current in power systems and conduction losses in wirings and transformers [1]. As a result, it may damage or shorten the equipment's lifespan.

In contrast, the nonlinear loads need a nonsinusoidal supply current waveform. Thus, other than lowering the input PF, the loads increase the supply current's total harmonic distortion (THD) value. It is due to the switching operation of the semiconductor power converters; they generate high harmonic components into the supply current waveform. Consequently, the high THD value can also increase the power system's current. Furthermore, the high-frequency harmonic components generated can contribute to an additional core loss in motors and interfere with the frequency of nearby communication lines [2].

Generally, a radial electrical system has multiple linear and nonlinear loads connected to the same Point of Common Coupling (PCC). The combination of both loads is known as composite loads [3]. However, since the nonlinear loads cause the adverse quality of the supply current waveshape, it may affect the operation of the linear loads. The effect becomes severe to loads highly sensitive to the change of the supply current waveform. Among all mitigation tools, a Shunt Active Power Factor (SAPF) can mitigate both high THD and low PF simultaneously [4]. The filter injects harmonic current and reactive power to compensate for harmonic components and reactive power supplied by an AC source.

An RL filter is commonly employed to filter the SAPF's injection current. It is connected to the PCC on the SAPF's AC side [5][6][7]. Moreover, to escalate compensation performance, other RL filters can be connected to the PCC on the AC source side only [8][9][10], the load side only [11][12][13] or the AC source and load sides [2][7][8]. However, no publication has highlighted the RL filters' significance and consequences before and after the SAPF installation. Especially the effect of RL filters connected to the PCC on the AC source or load side on the load current waveform and its properties. Nevertheless, this paper is interested in only studying the effect of the RL filter connected to the load side. It focuses on the SAPF performance without and with the RL filter, the effect of the RL filter on the load current waveform, and its properties.

Manuscript received on 05 September 2022 | Revised Manuscript received on 07 September 2022 | Manuscript Accepted on 15 November 2022 | Manuscript published on 30 November 2022.

***** Correspondence Author (s)
Nor Farahaaida Abdul Rahman*, School of Electrical Engineering, College of Engineering, Universiti Teknologi MARA, Shah Alam, Selangor, Malaysia. Email: farahaida@uitm.edu.my

Other than that, for the last three years (2019 – 2021), many scholars have been conducting research to enhance SAPF performance. There are five categories of those research work: (i) control algorithms/ controllers [6][7][9][12][14][16][17][18], (ii) SAPF topologies/ converters [5][16][19][20][21], (iii) SAPF for specific loads/ applications and performance analysis [8][10][22][23][24], (iv) Optimisation techniques [5][15][19][25], and (v) extraction algorithms [7][11][13].

In the first category, authors in [6], [7], [16] and [17] focus on enhancing SAPFs' current controllers. They introduced a three-level hysteresis controller [6], a Proportional Integral (PI) controller with integral windup action, a neuro-fuzzy controller based on the Adaptive Neuro-Fuzzy Inference System (ANFIS) [16], and a one-cycle digital controller for minimising the integral error [17]. Instead, authors in [9], [12], [14] and [18] focus on improving the control algorithm itself. The authors in [9] introduced a Finite Impulse Response (FIR) predictor controller to a digital microcontroller. It causes the microcontroller to have one sampling period delay only. Meanwhile, the authors in [12] presented a modulated model based on Pareto-based MO-M2 predictive control that can be adapted to any converter topology. In comparison, the authors in [16] presented an improved Predictive Direct Power Control (PDPC) algorithm. Finally, the authors in [18] developed a double closed looped current control algorithm to adapt weak grid application.

Several inverter topologies based on SAPF operation have been introduced in the second category. There are three-phase Flying Capacitor Inverter (FCI) [5], neutral point clamped (NPC) [16], five-level cascaded H-bridge (CHB) inverter [19], 13-level cascaded H-bridge (CHB) converter [20], and shunt isolated active power filter with common dc link integrating braking energy recovery [21]. Some topologies were introduced to satisfy particular standards, such as the NRS 048-2:2003 grid code standard [19], and to minimise the THD value [20].

Despite converter topologies, in category three, some SAPFs were developed for specific applications, systems or loads. Such as an unbalance load system [8], medium and high power brushless DC (BLDC) motor drives [10], Induction Heating (IH) system [22], and varied power supply source and load parameters [23]. Meanwhile, the authors in [24] introduced a singular perturbation technique, and averaging theory is used for a complete and rigorous formal analysis to describe the control system performances.

In recent years, some researchers introduced several optimisation techniques (in category four) to enhance the existing control algorithms or controllers. For example, the authors in [5], [15] and [19] designed an Artificial Neural Network based on Particle Swarm Optimisation (ANN-PSO) to improve a SAPF's current control algorithm. They utilised it to obtain optimal control parameters to satisfy power quality requirements and high dynamic responses [15]. Meanwhile, the authors in [19] used the optimisation technique to perform the Selective Harmonic Minimisation-Pulse Amplitude Modulation (SHM-PAM) technique utilising the least number of switching based on the optimised waveform pattern. Instead, the authors in [25] developed an algorithm for finding the optimal control for a current controller that operates as a part of a SAPF control system.

Lastly, few researchers tried to improve SAPF extraction techniques. In [7] and [13], the authors introduced an extraction algorithm based on the modified power balance theory [7] and the adaptive linear neural network approach [13]. Meanwhile, the authors in [11] implemented an Adaptive Notch Filter (ANF) to extract the reference signal.

However, most researchers focus on applying a SAPF for a single nonlinear load except the authors of the following papers: [6][8][13][21] and [23].

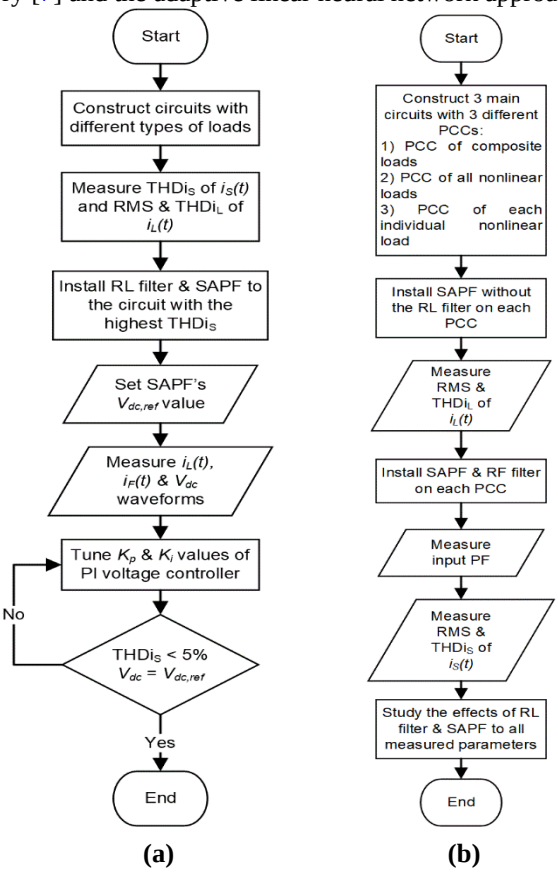

Fig. 1. Flowcharts of phases (a) and (b) procedures.

Table- I: Parameters of components used in the simulation work

Description	Component	Value
Main power supply	AC source	220 V & 50 Hz
RL LL	Resistor Inductor	80 Ω 50 mH
RL NL	Rectifier Resistor Inductor	 80 Ω 50 mH
RLC NL	Rectifier Resistor Inductor Capacitor	 80 Ω 50 mH 450 µF
RC NL	Rectifier Resistor Capacitor	 80 Ω 450 µF
RL filter	Resistor, R Inductor, L	1 Ω 5 mH
SAPF	Resistor, R_F Inductor, L_F DC-link capacitor, C	0.1 Ω 8 mH 2200 µF

Even for the past ten years, there have been very few publications related to SAPFs for a system consisting of a combination of nonlinear loads or composite loads [3][26][27][28]. Nevertheless, all of them utilised a single SAPF (centralised) to compensate for harmonic components generated by the loads. The centre of attention of their results is the effectiveness of the SAPF for compensating the harmonic components and reactive power. Despite that, the effect of using the centralised SAPF on the linear load in the system is not subjective studied. Therefore, the authors of [29] published a work that studies the effect of using centralised and individual SAPFs on the supply current and linear load current waveforms in the radial electrical system. However, they only consider the waveshape of both current waveforms, THD values and harmonic components; there is no study on the rms current and input PF. Thus, this paper will continue the study by considering the above parameters. Additionally, unlike in [29], this work will study the effect of installing single-phase SAPFs at different PCCs.

The paper has four sections: the introduction presents the background study, literature review, problem statements and objectives, the methodology explains all procedures executed to achieve the objectives, the results and discussions verify the centralised and individual SAPFs operation regarding three case studies, and the conclusion summaries the results according to the objectives.

II. METHODOLOGY

Fig. 1 shows the procedures of the research work. It has two phases: (a) constructing and tuning the SAPF's circuit and control algorithm and (b) investigating the effect of the RL filter and the single-phase centralised and individual SAPFs on the supply and load current waveforms and their properties.

A. Phase A

This work considers four types of loads: Inductive Linear Load (RL LL) and Inductive Nonlinear Load (RL NL), Inductive-Capacitive Nonlinear Load (RCL NL), and Capacitive Nonlinear Load (RC NL). All nonlinear loads consist of single-phase uncontrollable rectifiers with passive elements. Table I presents the parameters of those loads.

Initially, Matlab/ Simulink simulates each load separately with a single-phase AC source for measuring the rms and THD values of the instantaneous supply current $i_S(t)$. Then, a single-phase SAPF is constructed and tuned according to the circuit with the highest $i_S(t)$ THD value.

Fig. 2 depicts the RL filter and the SAPF's circuit and control algorithm. Fig. 2(a) indicates that the RL filter connects at the PCC of the load side, and the SAPF connects in parallel with the AC source. The current control algorithm utilises a bandless hysteresis controller, and the voltage control algorithm applies a PI controller. Both controllers regulate the instantaneous compensation current $i_F(t)$ and the dc-link voltage V_{dc}. The gains of the PI controller are tuned according to two indicators: (a) the V_{dc} value equals the

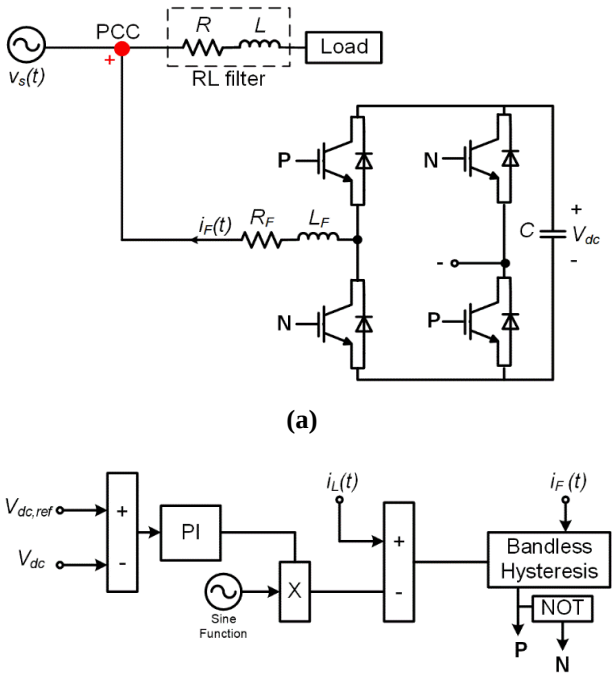

Fig. 2. Diagrams of (a) the RL filter and SAPF circuit and (b) SAPF control algorithm.

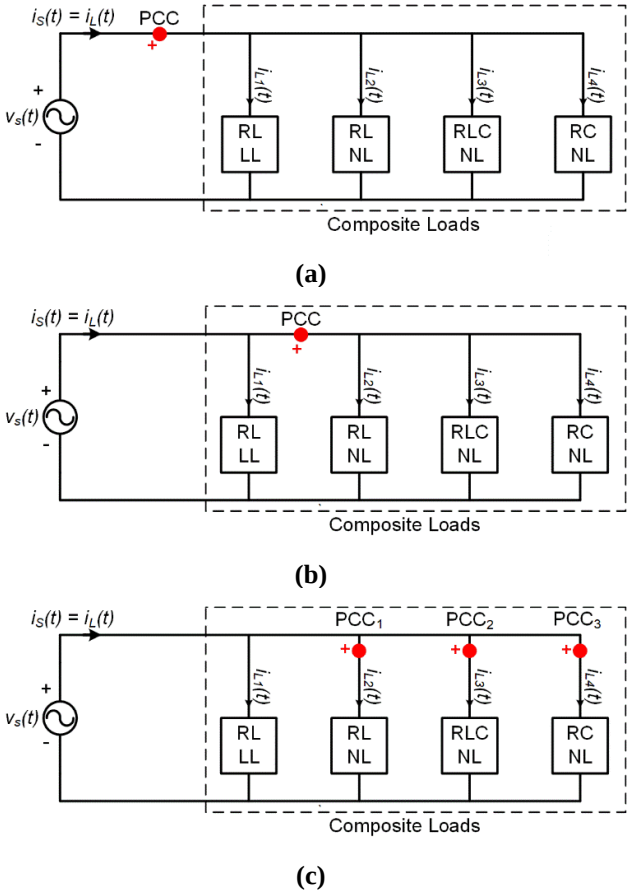

Fig. 3. PCCs in the primary radial circuits for Cases (a) 1, (b) 2 and (c) 3.

Published By:
Blue Eyes Intelligence Engineering and Sciences Publication (BEIESP)

reference dc-link voltage $V_{dc,\ ref}$, and (b) the $i_S(t)$ THD value below 5% (according to the IEEE Standard 519-2014). Table I tabulates the parameter value of the RF filter and the SAPF.

B. Phase B

In this phase, three primary radial circuits are constructed using the loads in Table I. Each circuit has different PCCs for installing the RF filter and the SAPF. All circuits are utilised for three case studies. Case 1 focuses on the effect of the RL filter and a centralised SAPF installed at the PCC of the composite loads. Other than the effect of the RL filter, Case 2 still considers the centralised SAPF implementation. However, the PCC is now at the connection point of all nonlinear loads. Meanwhile, Case 3 focuses on the individual SAPFs connected to each nonlinear load. Fig. 3 shows the configuration and PCCs of each primary circuit. This work applies the same SAPF in the previous phase as the centralised and individual SAPFs, regardless of the case studies. Firstly, all primary circuits only apply the SAPFs for investigating the necessity of the RL filter. The parameter involved in this investigation is $i_S(t)$ only. Then, the primary circuits only utilise the RF filter. The filter is installed on each PCC and in series with the dedicated loads. In this stage, the analysis involves the measurement of the rms and THD values of the instantaneous composite $i_L(t)$, RL LL $i_{L1}(t)$, RL NL $i_{L2}(t)$, RCL NL $i_{L3}(t)$, and RC NL $i_{L4}(t)$ current waveforms. The study also considers the input PF, the rms and THD values of $i_S(t)$. Lastly, the primary circuits use both the RF filters and SAPFs. In the last stage, the analysis focuses on the same parameter as the previous stage, except for the load currents.

III. RESULTS AND DISCUSSIONS

This section refers to Fig. 1(a) in arranging and discussing all results obtained from the simulation work. It considers four operating conditions for each study case: all primary radial circuits operate (1) without the RL filters and SAPFs, (2) with the SAPFs only, (3) with the RF filters only, and (4) with the RL filters and SAPFs.

A. Operating Condition 1 (no filters implementation)

Table II presents the rms and THD values of both supply and loads current waveforms. Regardless of the study cases,

$$i_S(t) = i_L(t). \quad (1)$$

Table II indicated that each load drew a different rms current value; RCL NL and RC NL drew a higher rms current value than RL LL and RL NL. Hence, it increased the rms supply current value. In addition, according to the THD values, the presented data depicted that the capacitive nonlinear loads generated higher harmonic components in the load current waveform than the inductive nonlinear load. In contrast, the inductive linear load did not generate any harmonic component. Hence, it justified that the $i_{L2}(t)$, $i_{L3}(t)$ and $i_{L4}(t)$ waveforms were distorted from the sinusoidal waveshape, and the $i_{L1}(t)$ waveform was purely sinusoidal. Therefore, it has been proven that the primary source of the harmonic problem was the nonlinear loads.

B. Operating Condition 2 (SAPFs implementation)

Fig. 4 depicts all case studies' compensated $i_S(t)$ waveforms. The waveforms in all figures demonstrated that the SAPFs could perform harmonic compensation regardless

Table- II: RMS and THD values of all current waveforms

Parameters	$i_S(t) = i_L(t)$	$i_{L1}(t)$	$i_{L2}(t)$	$i_{L3}(t)$	$i_{L4}(t)$
RMS, A	19.93	2.697	2.688	8.38	8.402
THD, %	92.55	0	8.09	139.09	139.43

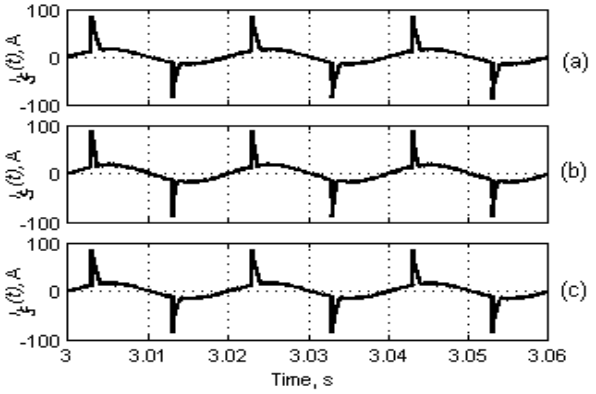

Fig. 4. Compensated $i_s(t)$ waveforms when the SAPFs operate without the RL filters in Cases (a) 1, (b) 2 and (c) 3.

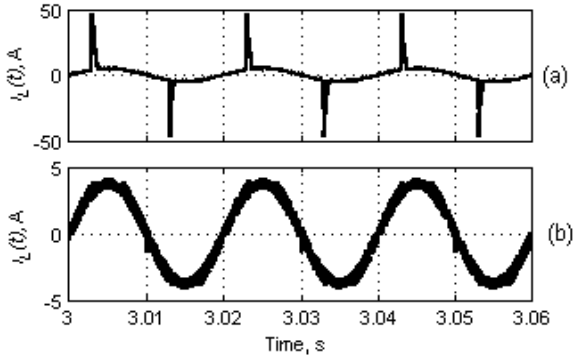

Fig. 5. Compensated $i_s(t)$ waveforms when the SAPFs operate without the RL filters. The primary circuit connects to (a) Load 4 (high THD value) or (b) Load 2 (low THD value) only.

of the study cases. However, the current waveforms had high current spikes in both positive and negative half-cycles. It happened due to the compensation of very high harmonic components. Fig. 5 shows the compensated $i_S(t)$ waveforms when the AC source supplies an individual load that generates either the highest or lowest harmonic components. The waveforms verified that the current spike positively correlated with the harmonic components. Therefore, the RF filter is necessary when installing SAPFs.

C. Operating Condition 3 (RF filters implementation)

The study focuses on the effect of using the RF filters on the rms and THD values of $i_L(t)$, $i_{L1}(t)$, $i_{L2}(t)$, $i_{L3}(t)$, and $i_{L4}(t)$. Table III and IV present the rms and THD values of all current waveforms for all case studies. The discussion started with the effects of the RL filters on the composite load current ($i_L(t)$), linear load current ($i_{L1}(t)$) and nonlinear load currents ($i_{L2}(t)$, $i_{L3}(t)$, and $i_{L4}(t)$).

Table- III: Percentage different of rms load current values without and with the RL filter

	Case 1	Case 2	Case 3
$i_L(t)$	- 0.27%	- 0.25%	- 0.16%
$i_{L1}(t)$	- 0.08%	0	0
$i_{L2}(t)$	- 0.08%	- 0.06%	- 0.02%
$i_{L3}(t)$	- 0.38%	- 0.38%	- 0.26%
$i_{L4}(t)$	- 0.38%	- 0.37%	- 0.26%

Table- IV: Percentage different of load current THD values without and with the RL

	Case 1	Case 2	Case 3
$i_L(t)$	- 0.56%	- 0.55%	- 0.42%
$i_{L1}(t)$	1211 %	0	0
$i_{L2}(t)$	0.79 %	0.82%	- 0.35%
$i_{L3}(t)$	- 0.51%	- 0.51%	- 0.40%
$i_{L4}(t)$	- 0.50%	- 0.51%	- 0.40%

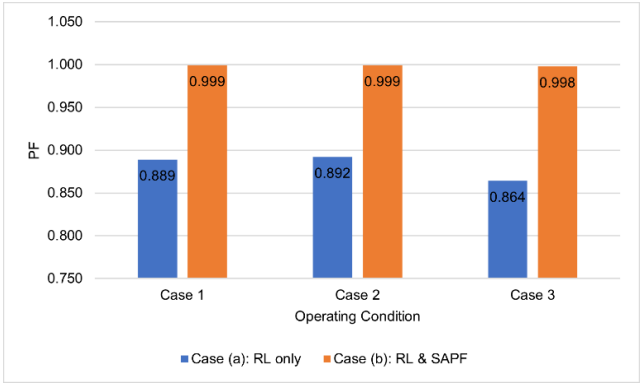

Fig. 6. Effects of the RL filters and SAPFs on the input PF.

According to Table III, the $i_L(t)$ rms values reduced between 0.16% to 0.27%. Similarly, based on Table IV, the $i_L(t)$ THD values decreased between 0.42% to 0.56%. However, due to the slight drop in the rms and THD values, thus, the RF filters did not affect the current draws by the composite load significantly.

In contrast, Table III indicated that the $i_{L1}(t)$ rms values remain unchanged in Cases 2 and 3 but in Case 1. Nevertheless, the change in Case 1 was minimal, which was 0.08% and can be negligible. In addition, Table IV revealed that the RF filters tremendously afflicted the $i_{L1}(t)$ THD value in Case 1. The value increased by 1211%. Hence, it has been proven that the RL filters have changed the $i_{L1}(t)$ waveform from a purely sinusoidal to a distorted sinusoidal wave shape. However, the THD values remind unchanged for Cases 2 and 3. Unlike Cases 2 and 3, the RL filter in Case 1 (Fig. 3(a)) connected to the PCC before RL LL. Thus, it affected the shape of the current drawn by the linear load. Therefore, the RF filters are not suitable to be connected before the linear load because they can adversely distort the wave shape of the current waveform.

Similar to the $i_L(t)$ and $i_{L1}(t)$ waveforms, Table III exhibited that the rms values of all nonlinear load currents

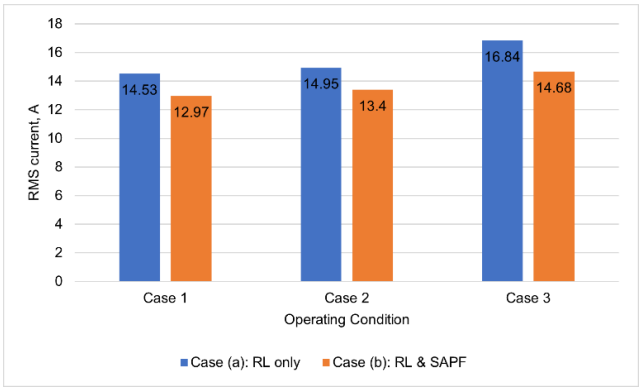

(a)

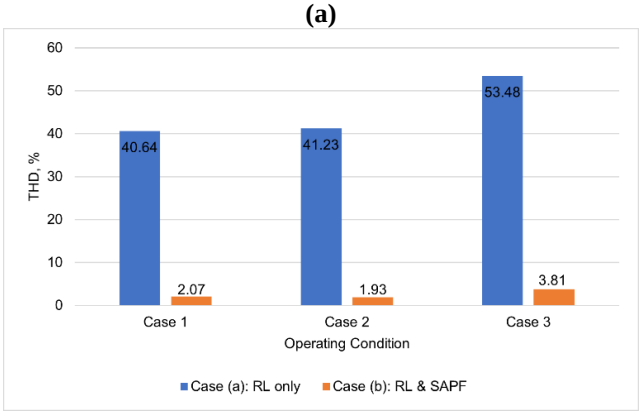

(b)

Fig. 7. Effects of the RL filters and SAPFs on the $i_S(t)$ (a) RMS and (b) THD values.

dropped slightly from 0.02% to 0.08% for $i_{L2}(t)$, and 0.26% to 0.38% for $i_{L3}(t)$ and $i_{L4}(t)$. Hence, it demonstrated that the RL filter caused a significant effect on the capacitive nonlinear loads (RLC LL and RC LL) instead of the inductive nonlinear load (RL LL). The effect was noticeable since RLC LL and RC LL drew higher currents than RL LL. Nonetheless, as shown in Table IV, the filters affected the THD values of all nonlinear loads' currents differently. For RL LL, the $i_{L2}(t)$ THD values increased around 0.8% in Cases 1 and 2 and decreased to 0.35% in Case 3. It happened due to multiple connections of RL filters at three PCCs, and the load drew a small current. For RCL LL and RC LL, the $i_{L3}(t)$ and $i_{L4}(t)$ THD values decreased from 0.4% to 0.5%, regardless of case studies. Nonetheless, the changes in the THD values for both inductive and capacitive nonlinears' currents are small and insignificant.

D. Operating Condition 4 (RF filters and SAPFs implementation)

Figs. 6 to 8 present the value of the input PF, the rms and THD of $i_S(t)$ when the primary radial circuits apply the individual RF filters and the combination of the filter and SAPFs. According to the simulation work, the input PF of all primary circuits without both filters was 0.719. However, Fig. 6 indicated that both filters could increase the PF. Nonetheless, the circuits required both filters to achieve the unity PF. Hence, it has been proven that combining the RF filters and SAPFs could improve the input PF.

Based on the relationship between $i_S(t)$ and $i_L(t)$ discussed in (1) and Fig. 6, the RF filter installation could also reduce the $i_S(t)$ rms value. Nevertheless, Fig. 7(a) revealed that the combination of the RF filters and SAPFs had further reduced the $i_S(t)$ rms values. The values dropped around 10% to 13% since the impedance catered by the AC source increased due to the composite loads, RF filters and SAPFs.

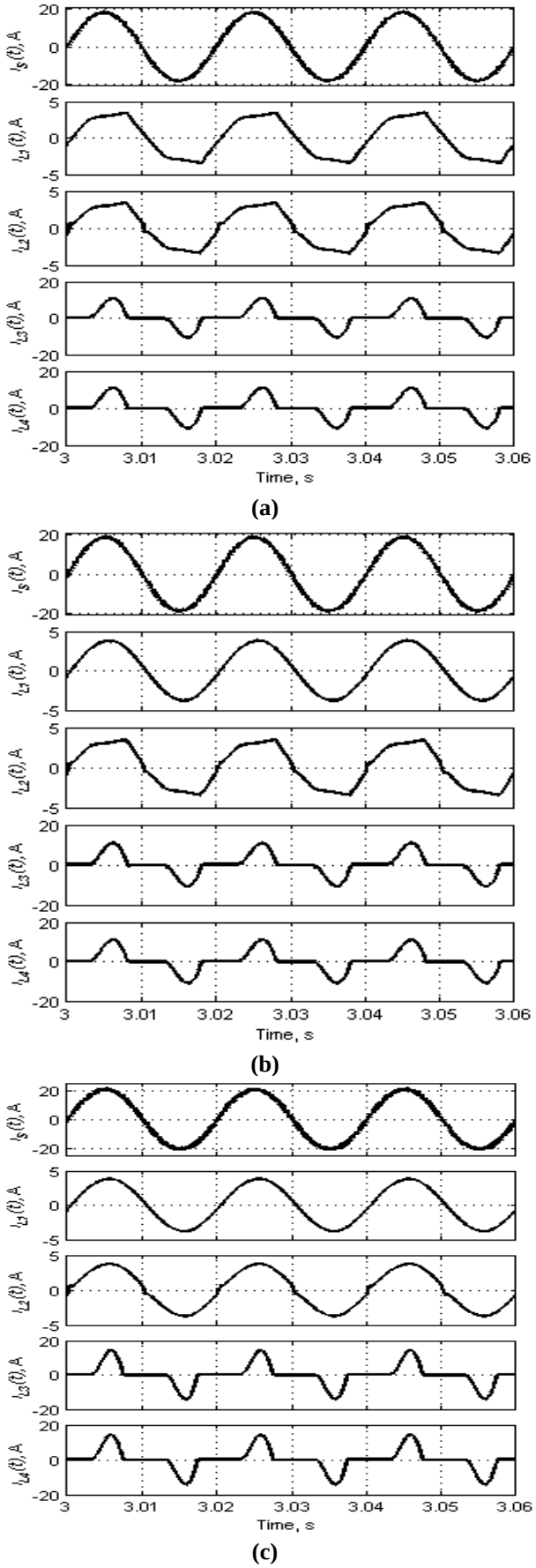

Fig. 10. Waveforms of all instantaneous currents after the RL filters and SAPFs installation in Case (a) 1, (b) 2, and (c) 3.

Additionally, Fig. 7(b) showed that the RF filters reduced the $i_S(t)$ THD values from 92.55% (Table II for $i_L(t)$) to 40% to 53%. Subsequently, the value decreased to below 5% after the SAPFs implementation. Hence, it exhibited that the function of the RF filters was to reduce the $i_S(t)$ THD values before the SAPFs could perform extensive harmonic compensation. Therefore, all $i_S(t)$ THD values presented have complied with the IEEE Standard 519-2014. Moreover, Fig. 7(b) indicated that both filters compensated harmonic currents more effective in Cases 1 and 2 than in Case 3. Thus, it justified that the centralised SAPFs could perform better than the individual SAPFs. The factors on why the individual SAPFs cannot perform better were related to the increase in the number of the SAPFs' impedance and control algorithms.

Nonetheless, as the continuation of the effect of the RL filters in Operating Condition 3, the installation of the SAPF in Case 1 could not rectify the distorted linear current waveform. Therefore, installing a centralised SAPF at the PCC that has composite loads is not recommended. Instead, it is suitable to group all nonlinear loads at one PCC for the filter installation to avoid any linear load current waveform deterioration, such as in Case 2. Fig. 8 shows the waveforms of all instantaneous currents in all case studies after the filter installation. The figures validate all the previous discussions.

IV. CONCLUSION

According to the simulation results, SAPFs require RL filters to operate effectively. However, the filters could alter the load current waveform and its properties. Nonetheless, the changes are small, and they can be considered negligible. Additionally, the simulation results verify that the centralised SAPFs are more suitable for the radial electrical system. The SAPFs must only be installed at the PCC of nonlinear loads to avoid linear load current waveform distortion.

ACKNOWLEDGMENT

The research was supported by Universiti Teknologi MARA (UiTM) under Lestari Grant 600-RMC/MYRA 5/3/ LESTARI (037/2020) & the College of Engineering UiTM.

REFERENCES

1. L. Cividino, "Power factor, harmonic distortion; causes, effects and considerations" [Proceedings] Fourteenth International Telecommunications Energy Conference - INTELEC'92, 1992, pp. 506-513, doi: 10.1109/INTLEC.1992.268395. [CrossRef]
2. A. Ganiyu Adedayo, and O. Adedapo Ibukunoluwa, "Effects of total harmonic distortion on power system equipment," Innovative Systems Design and Engineering, vol. 6, no. 5, pp. 114-120, 2015: https://iiste.org/Journals/index.php/ISDE/article/view/22744
3. N. Patnaik and A. K. Panda, "Comparative analysis on a shunt active power filter with different control strategies for composite loads" TENCON 2014 - 2014 IEEE Region 10 Conference, 2014, pp. 1-6, doi: 10.1109/TENCON.2014.7022289. [CrossRef]

4. P. Salmerón Revuelta, S. Pérez Litrán, J. Prieto Thomas, "Active power line conditioners," design, simulation and implementation for improving power quality, (), 231–284. doi:10.1016/b978-0-12-803216-9.00007-9. [CrossRef]
5. D. Khaled, A. Tayeb, C. Gerard, D. Mouloud, and H. Chaib, "Particle swarm optimisation trained artificial neural network to control shunt active power filter based on multilevel flying capacitor inverter," European Journal of Electrical Engineering, vol. 22, no. 3, pp. 199 – 207, June 2020, doi: 10.18280/ejee.220301. [CrossRef]
6. P. Balamurugan, and N. Senthil Kumar, "Three level hysteresis function based sliding mode control of three phase PWM inverter for shunt active power filter application in distribution network," International Journal of Recent Technology and Engineering, vol. 8, no. 3, pp. 8015 – 8019, September 2019, doi: 10.35940/ijrte.C6416.098319. [CrossRef]
7. K. Khechiba, L. Zellouma, and A. Kouzou, "PI regulator with tracking anti-windup based modified power balance theory for SAPF under unbalanced grid voltage unbalance non linear loads," Electronics, vol. 23, no. 2, pp. 75 – 80, 2019, doi: 10.7251/ELS1923075K. [CrossRef]
8. B. Karim Belalia, K. Mohammed, B. Hamid, B. Azeddine, and M. Abdelkader, "Network current quality enhancement under nonlinear and unbalanced load conditions using a four-wire inverter-based active shunt filter," Indonesian Journal of Electrical Engineering and Informatics, vol. 9, no. 3, pp. 601 – 614, September 2021, doi: 10.52549/.V9I3.2951. [CrossRef]
9. O. Kukrer, H. Komurcugil, R. Guzman, and L. G. De Vicuna, "A new control strategy for three-phase shunt active power filters based on FIR prediction," IEEE Transactions on Industrial Electronics, vol. 68, no. 9, pp. 7702 – 7713, September 2021, doi: 10.1109/TIE.2020.3013761. [CrossRef]
10. S. Kumaresan, and H. Habeebullah Sait, "Design and control of shunt active power filter for power quality improvement of utility powered brushless dc motor drives," Automatika, vol. 61, no. 3, pp. 507 – 521, July 2020, doi: 10.1080/00051144.2020.1789402. [CrossRef]
11. M. Syahrul Hisham, M. R. Mohd Amran, M. Nashiren Farzilah, A. W. Noor Izzri, J. Auzani Jidin, and Y. L. Musa, "Adaptive notch filter under indirect and direct current controls for active power filter," Bulletin of Electrical Engineering and Informatics, vol. 9, no. 5, pp. 1794 – 1802, October 2020, doi: 10.11591/eei.v9i5.2165. [CrossRef]
12. P. Santis, D. Sáez, R. Cárdenas, and A. Núñez, "Pareto-based modulated model predictive control strategy for power converter applications," Electric Power Systems Research, vol. 171, pp. 158 – 174, June 2019, doi: 10.1016/j.epsr.2019.02.016. [CrossRef]
13. Y. Hoon, M. A. Mohd Radzi, A. S. Al-Ogaili, "Adaptive linear neural network approach for three-phase four-wire active power filtering under non-ideal grid and unbalanced load scenarios," Applied Sciences (Switzerland), vol. 9, no. 24, pp. 1-25, December 2019, doi: 10.3390/app9245304. [CrossRef]
14. Y. Bekakra, L. Zellouma, and O. Malik, "Improved predictive direct power control of shunt active power filter using GWO and ALO – Simulation and experimental study," Ain Shams Engineering Journa, vol. 12, no. 4, pp. 3859 – 3877, December 2021, doi: 10.1016/j.asej.2021.04.028. [CrossRef]
15. O. Gherouat, A. Hassam, O. Aissa, and B Babes, "Experimental evaluation of single-phase shunt active power filter based on optimized synergetic control strategy for power quality enhancement," Journal Européen des Systèmes Automatisés, vol. 54, no. 4, pp. 649-659, August 2021, doi: 10.18280/jesa.540415. [CrossRef]
16. M. M. Tounsi, A. Allali, H. M. Boulouiha, and M. Denaï, "ANFIS control of a shunt active filter based with a five-level NPC inverter to improve power quality," International Journal of Electrical and Computer Engineering, vol. 11, no. 3, pp. 1886 – 1893, June 2021, doi: 10.11591/ijece.v11i3.pp1886-1893. [CrossRef]
17. S. Orts-Grau, P. Balaguer-Herrero, J.C. Alfonso-Gil, C. I. Martínez-Márquez, F. J. Gimeno-Sales, S. Seguí-Chilet, "One-cycle zero-integral-error current control for shunt active power filters," Electronics (Switzerland), vol. 9, no. 12, pp. 1 – 16, December 2020, doi: 10.3390/electronics9122008. [CrossRef]
18. J. Wang, F. Xu, Fanga, G. Pan, K. Ouyang, Y. Jin, L. Libin, and J. Qiu, "Robust control method for LCL-type shunt active power filter under weak grid condition," IET Generation, Transmission and Distribution, vol. 14, no. 11, pp. 2120 – 2128, June 2020, doi: 10.1049/iet-gtd.2019.1381. [CrossRef]
19. S. Kundu, S. Banerjee, and S. Bhowmick, "Improved SHM-PAM-based five-level CHB inverter to fulfil NRS 048-2:2003 grid code and to apply as shunt active power filter with tuned proportional-resonant controller for improving power quality," IET Power Electronics, vol. 13, no. 11, pp. 2350 – 2360, August 2020, doi: 10.1049/iet-pel.2019.1295. [CrossRef]
20. V. Narasimhulu, D. V. Ashok Kumar, and Ch. Sai Babu, "Recital analysis of multilevel cascade H-bridge based active power filter under load variation," SN Applied Sciences, vol. 1, no. 12, December 2019, doi: 10.1007/s42452-019-1669-8. [CrossRef]
21. H. Liu, C. Li, Z. Zheng, J. Liu and Y. Li, "Shunt isolated active power filter with common dc link integrating braking energy recovery in urban rail transit" in IEEE Access, vol. 7, pp. 39180-39191, 2019, doi: 10.1109/ACCESS.2019.2906329. [CrossRef]
22. R. Rahul, D. Subrata Kumar, S. Priya, D. Mrigakshi, S. Amarjit, and S. Pradip Kumar, "Feasible evaluation of shunt active filter for harmonics mitigation in induction heating system," High Tech and Innovation Journal, vol. 2, no. 3, pp. 235 – 245, September 2021, doi: 10.28991/HIJ-2021-02-03-08. [CrossRef]
23. S. Yuriy, A. Boris, and P. Veronika, "The assesement of the shunt active filter efficiency under varied power supply source and load parameters," International Journal of Electrical and Computer Engineering, vol. 10, no. 6, pp. 5621 – 5630, December 2020, doi: 10.11591/ijece.v10i6.pp5621-5630. [CrossRef]
24. Y. Mchaouar, C. Taghzaoui, A. Abouloifa, M. Fettach, A. Ellali, I. Lachkar, and F. Giri, "Sensorless nonlinear control strategy of the single phase active power filters via two-time scale singular perturbation technique," Universal Journal of Electrical and Electronic Engineering, vol. 6, no. 5, pp. 383 – 401, 2019, doi: 10.13189/ujeee.2019.060509. [CrossRef]
25. K. Kołek, and A. Firlit, "A new optimal current controller for a three-phase shunt active power filter based on Karush–Kuhn–Tucker conditions," Energies, vol. 14, no. 19, October-1 2021, pp. 1-17, doi: 10.3390/en14196381. [CrossRef]
26. Z. F. Hussien, N. Atan and I. Z. Abidin, "Shunt active power filter for harmonic compensation of nonlinear loads," Proceedings. National Power Engineering Conference, 2003. PECon 2003., 2003, pp. 117-120, doi: 10.1109/PECON.2003.1437429. [CrossRef]
27. C. Nalini Kiran, D. Subhransu Sekhar, and S. Prema Latha, "A few aspects of power quality improvement using shunt active power filter," International Journal of Scientific & Engineering Research, vol. 2, no. 5, pp. 1-11, May 2011.
28. Z. Zehara, and P. Nishant, "Power quality improvement by using shunt active power filter," International Journal for Research in Applied Science & Engineering Technology (IJRASET), vol. 7 no. VI, pp. 2255-2260, June 2019, doi: 10.22214/ijraset.2019.6378. [CrossRef]
29. N. A. Rahman and N. Sa'adon, "Centralised and individual shunt active power filters in radial electrical systems," 2021 IEEE Industrial Electronics and Applications Conference (IEACon), 2021, pp. 62-66, doi: 10.1109/IEACon51066.2021.9654480. [CrossRef]

AUTHORS PROFILE

Nor Farahaida Abdul Rahman, is working as a senior lecturer at the School of Electrical Engineering, College of Engineering, Universiti Teknologi MARA, 40450 Shah Alam, Selangor, Malaysia. She received her B.Eng. (Hons.) and M.Eng. degrees from Universiti Teknologi Malaysia (UTM), and a PhD in Power Engineering from Universiti Putra Malaysia (UPM). Her research interests are active filters, power quality and power electronics.